Elimination of H_2 from $CH_3CH=N^+HCH_3$: A Synchronous, Concerted 1,4-H_2 Elimination

Charles E. Hudson,[a] Richard D. Bowen,[b] and David J. McAdoo[a]

[a] Department of Neuroscience and Cell Biology, University of Texas Medical Branch, Galveston, Texas, USA
[b] Division of Chemical and Forensic Sciences, School of Life Sciences, University of Bradford, West Yorkshire, United Kingdom

Most H_2 eliminations from cations in the gas phase are formally 1,1- or 1,2- processes. Larger ring size H_2 eliminations are rare and little studied. Thus, whether the 6-center, 1,4-elimination $CH_3CH=N^+HCH_3 \rightarrow CH_2=CHN^+H=CH_2 + H_2$ is concerted and synchronous, as indicated by isotope effects and predicted by conservation of orbital symmetry, is a significant question. This reaction is characterized here by application of QCI and B3LYP theories. CH bond-breaking and H–H bond-making in this reaction are found by theory to be highly synchronized, consistent with previously established isotope effects and in contrast to "forbidden" 1,2-eliminations from organic cations in the gas phase. This reaction is made feasible by its conservation of orbital symmetry, the energy supplied by formation of the H–H bond, and a favorable geometry of the ion for eliminating H_2. (J Am Soc Mass Spectrom 2008, 19, 27–32) © 2008 American Society for Mass Spectrometry

Most H_2-eliminations from cations in the gas-phase are 1,1- or 1,2-processes [1]. Near threshold, $CH_2=ND_2^+$ and $CD_2=NH_2^+$ both eliminate HD with high selectivity [1], demonstrating that they undergo a formal 1,2-elimination. H_2 eliminations from other $CH_2=ZH^+$ species (Z = O, S) have similar specificities [1]. However, 1,2 eliminations should violate conservation of orbital symmetry [2], conservation which opposes their synchronous occurrence. That such conservation can direct the course of a reaction is supported by alkane eliminations from ions avoiding orbital symmetry constraint by being generally stepwise, ion-neutral complex-mediated 1,2-processes rather than concerted eliminations [3, 4]. Substantial barriers to the reverse reactions of 1,2-H_2 eliminations are demonstrated by their production of broad, flat-topped metastable peaks. The reverse barriers to 1,2-eliminations of H_2 were first attributed to those reactions having to surmount high barriers imposed by conservation of orbital symmetry [5, 6]. However, theory later revealed that the transition-state geometries of many 1,2-eliminations strongly resemble CH_3Z^+, i.e., transition states of 1,1-eliminations [1, 7]. Presumably this route, although high in energy, is taken to circumvent orbital symmetry constraints [2]. In contrast to formal 1,2-eliminations, 1,1-eliminations often occur close to their thermochemical thresholds, demonstrating substantial differences in the reaction coordinates of these two types of reactions, despite their generation of the same products.

Although, as just described, 1,1- and 1,2-H_2-eliminations by cations are common and well characterized [1 and references therein], H_2-eliminations through larger ring sizes are rare and little studied. Therefore, to better understand such reactions, we characterize the 6-center elimination of H_2 from $CH_3CH=N^+HCH_3$ (1) in Scheme 1. This reaction is allowed by orbital symmetry, but gives a flat-topped metastable peak. The eliminations of H_2 from $CH_3CH=ND^+CH_3$ and HD from $CH_3CH=NH^+CD_3$ are highly selective (100% H_2 and 100% HD, respectively) [8], demonstrating that this reaction is a 1,4-elimination, a rare regioselectivity. Two of the five acyclic $C_3H_8N^+$ isomers eliminate H_2 by this route [8], as do $(CH_3)_2C=N^+HCH_3$ (3), $CH_3CH_2CH=NH^+CH_3$ (4), $CH_3CH_2CH=N^+(CH_3)_2$ (5), $(CH_3)_2C=N^+(CH_3)_2$ (6), and $CH_3CH_2CH_2CH=N^+(CH_3)_2$ (7) [9]. The 1,4-elimination of H_2 from 1 deserves further study because (1) it appears to be an orbital symmetry-allowed 6-electron cycloreversion with a relatively high-energy transition state, (2) parallel reactions are not observed in the fragmentation of any of the metastable oxonium ion homologs of 1 or any other family of ions, and (3) characterizing the synchronicity of the bond-making and bond-breaking steps, i.e., establishing whether the two C–H bonds that break do so sequentially or simultaneously, should add insight into what makes chemical reactions synchronous or asynchronous, a sometimes controversial issue [10, 11].
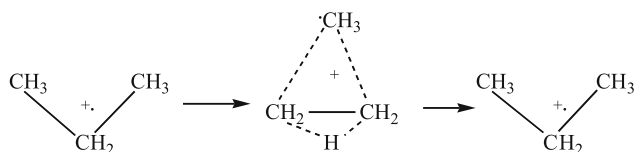
Bond-breaking and -making in concerted reactions of ions in the gas phase can be synchronous: for example, isomerization and dissociation of *n*-butane ions [12], of propane ions [13], and ethene elimination from $CH_3CH_2CH_2N^+H=CH_2$ [14] (Schemes 2, 3, and 4), or asynchronous: ethene elimination from $CH_3CH_2N^+H=$
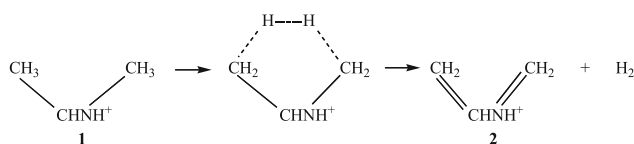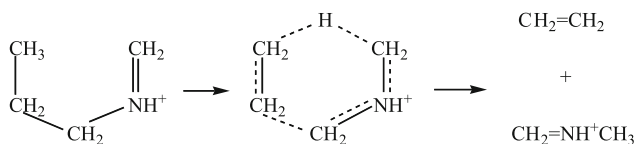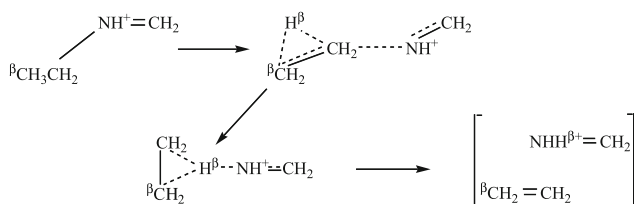
Scheme 1
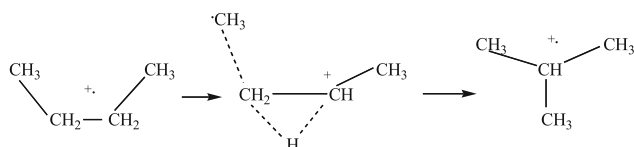
Scheme 2
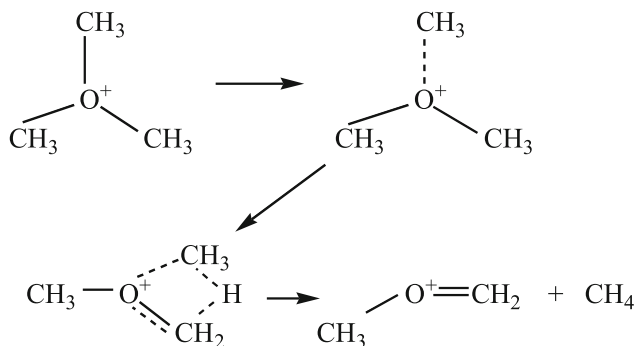

Scheme 3

Scheme 4

Scheme 5

Scheme 6

CH_2 [15] and methane elimination from $(CH_3)_3O^+$ [16] (Schemes **5** and **6**). In some synchronous reactions, the breaking of a bond is coupled to a simultaneous energetically downhill rearrangement, such as isomerization of primary carbocations to secondary or tertiary ones [3, 4, 12, 17]. Immonium ions such as **1**, the ion we study here, are of central importance in the Mannich reaction [18] and in the chemistry of enamines [19].

Scheme **2** depicts the isomerization of the *n*-butane cation to the 2-methylpropane cation. In this reaction, stretching of the C–C bond and the 1,2-H shift are synchronized [12].

Scheme **3** depicts the mechanism of isotopic exchange in the propane ion; this occurs by the simultaneous migration of a methyl group in one direction and an H in the other [13].

In Scheme **4**, 6-membered ring H-migration synchronized with C–C bond breaking eliminates ethene from
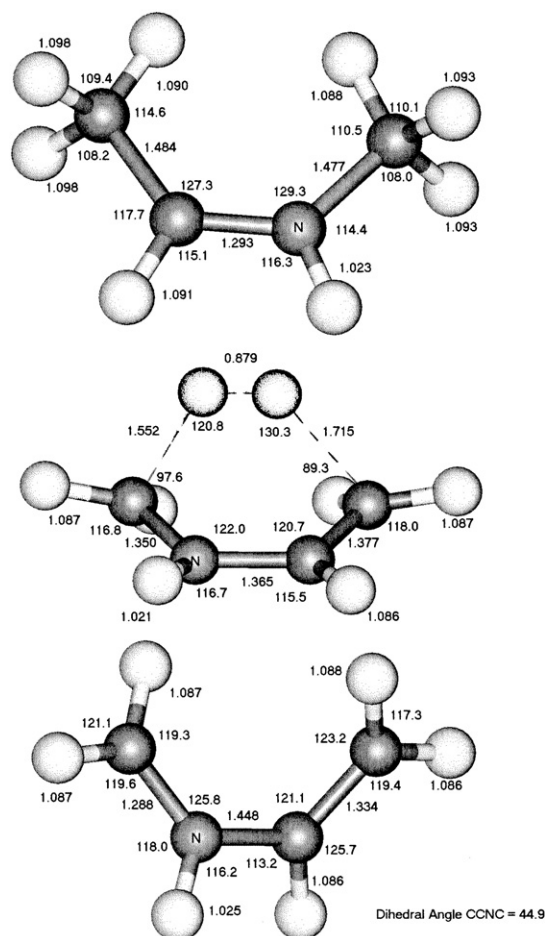
Figure 1. QCISD/6-31G(d) structures of cis-$CH_3CH=N^+HCH_3$ (**1**) (upper panel), the transition state for H_2-elimination from **1** (middle panel), and the product $CH_2=CHN^+H=CH_2$ (**2**) (bottom panel). In **1**, the heavy atoms and the uppermost hydrogens are all in the same plane, which bisects the remaining HCH bond angles. At the transition state, the H–H axis is parallel to the NC bond and H_2 is above the skeletal "plane". The cis product **2** was surprisingly twisted, the CCNC dihedral angle being 44.8°, the HCCH dihedral angle −136.6°, and the HNCH angle being −135.8°.

Figure 2. Changes in the lengths of CH and H–H bonds during the elimination of H_2 from $CH_3CH=NH^+CH_3$ (B3LYP theory). RC = reaction coordinate. The ground state ion is to the left and the dissociated products to the rig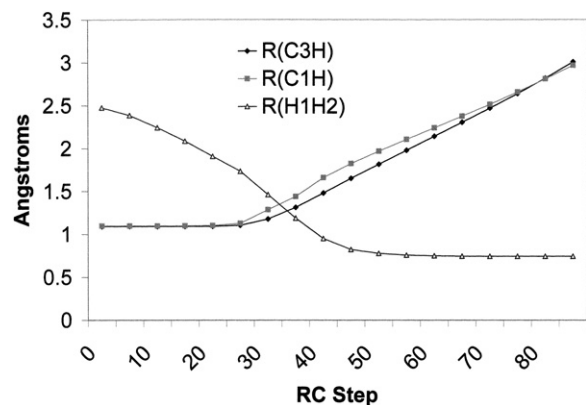ht ends of the traces in the figure. The units of the abscissa represent progress along the reaction coordinate. C1H is a CH bond in the methyl attached to C, and C3H is a CH bond in the methyl attached to N. The transition state occurs at step 43. Note that although the C1H bond is more extended than the C3H bond over much of the reaction, the extensions of the two bonds are substantially synchronized. The increasing distances between the hydrogens and carbons beyond the transition state are due to the separation of H_2 from the rest of the ion after the CH bonds are effectively broken.

$CH_3CH_2CH_2N^+H=CH_2$ [14]. This reaction is driven by its being energetically substantially downhill from the transition state.

Scheme **5** depicts asynchronous CN bond-breaking in $CH_3CH_2N^+H=CH_2$ before the migration of H from C^β to N to form a $[CH_2=CH_2\ NH_2^+=CH_2]$ complex [15].

In Scheme **6**, a CO bond is substantially stretched and weakened before H-transfer in the elimination of methane from the trimethyloxonium ion. H is transferred while the CO bond still possesses substantial covalent character, so it has been argued that this reaction is not concerted, although it also does not occur through an ion-neutral complex [16].

Theory

Energies (Tables 1 and 2) and geometries of stationary points were obtained using the Gaussian 03 program package [20]. Geometries were obtained by B3LYP/6-31G(d), B3LYP/6-311G(d,p) and QCISD/6-31G(d) theories and basis sets. Energies were obtained with the same levels of theory and basis sets as were the corresponding geometries, except QCISD(T)/6-311G(d,p) energies were obtained at QCISD/6-31G(d) geometries. Species were considered to be stable when they had only positive vibrational frequencies, and to be transition states when they possessed only one imaginary vibrational frequency. Zero point energies were obtained by multiplying zero point energies derived from B3LYP/6-31G(d) frequencies by Scott and Radom's scaling factor of 0.9806 [21]. Reaction pathways were

traced by intrinsic reaction coordinate (IRC) methods [22, 23] utilizing B3LYP theory and the 6-31G(d) basis set.

Results and Discussion

The Reaction Coordinate and Reaction Synchronicity

The geometries of cis-**1** (the reacting configuration), the transition state for H_2-elimination from **1**, and cis-$CH_2=CHNH^+=CH_2$ are given in Figure 1. The most stable conformation of **cis-1** has all of its atoms except two hydrogens of each methyl in a plane. For the out-of-plane hydrogens, the HCCN dihedral angles are 122.4° and −122.4°, and the out-of-plane HCNC dihedral angles are 120.5° and −120.6°). Thus the skeletal plane bisects the angles between both pairs of nonplanar hydrogens.

The skeleton remains nearly planar in the X-Y plane at the transition state (the CCNC dihedral angle = −4.07°). H_2 is formed by joining two hydrogens, one from each methyl, which project from the same side of the skeletal plane. According to QCISD/6-31G(d) theory, for the incipient H_2 hydrogens the HCCN dihedral angle = 43.9° and the HCNC dihedral angle = −43.7° at the transition state. Thus, the departing H_2 is outside the skeletal plane (Figure 1) with its axis parallel to that of the central C–N bond. There is little rotation of H_2 in any dimension during the course of the reaction. Both breaking CH bonds are considerably lengthened at the transition state, to 1.763 Å in the C-methyl and to 1.586 Å in the N-methyl versus 1.094 Å and 1.092 Å, respectively, in **1**. The H–H bond is substantially formed at the transition state (The H–H distance = 0.861 Å, compared with 0.746 Å for free H_2 according to QCISD/6-31G(d) theory). Thus, the energy supplied by forming H_2 (ca. 436 kJ mol⁻¹, the H–H bond energy) largely goes to break the NH and CH bonds. Ca. 282 kJ mol⁻¹, the critical energy for the H_2-elimination, is still required to reach the transition state. This is supplied by the excess energy in the system. This critical energy is substantial, in contrast to that for some *allowed* H_2-eliminations [1].

Somewhat surprisingly for a conjugated system, the cis product **2** was substantially twisted, the CCNC dihedral angle being 44.8°, the HCCH dihedral angle
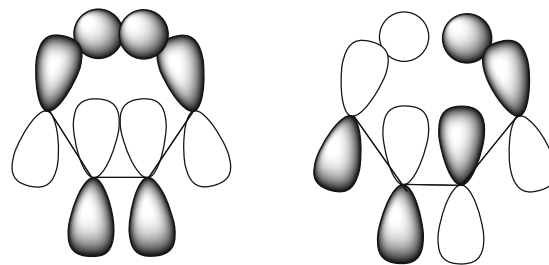

Figure 3. Orbitals drawn to reflect electron density distributions in the transition state for H_2-elimination from **1** generated by our computations.

Table 1. Energies for $CH_3CH=N^+HCH_3 \rightarrow CH_2=CHN^+H=CH_2 + H_2$ (hartrees)

Species	B3LYP/6-31G(d)	ZPVE	B3LYP/6-311g(d,p)	QCISD/6-31G(d)	QCISD(T)/6-311G(d,p)
Cis-**1**	-173.636091	286.3	-173.684464	-173.066973	-173.207265
Trans-**1**	-173.638952	286.2	-173.687164	-173.070017	-173.210099
TS, cis/ trans **1**	-173.534560	271.6	-173.583711	-172.959576	-173.101292
TS(-H$_2$)	-173.523258	266.8	-173.575648	-172.939344	-173.092447
s-cis **2**	-172.378044	226.0	-172.425924	-171.837634	-171.961312
s-trans **2**	-172.383729	226.2	-172.431486	-171.841289	-171.965080
H$_2$	-1.175482	26.1	-1.179571	-1.151698	-1.168336
TS(**1** → **1**′)		272.9	-173.574399		-173.095889

$-136.6°$ and the HNCH angle being $-135.8°$. This is probably due to steric effects, as similar twisting in neutral s-cis-1,3-butadiene is attributable to steric effects [24, 25]. For that species, we obtained the following values of the CCCC dihedral angle at different levels of theory: B3LYP/6-31G(d), B3LYP/6-31G(d), INT = ULTRAFINE, B3LYP/6-311G(d,p), and QCISD/6-31G(d): 30.3°, 30.2°, 32.9°, and 38.0°, respectively. In contrast, as expected, trans-**1** was planar, with a CNCC dihedral angle of 180.0°.

To obtain a more detailed description of the H$_2$-elimination, we traced the reaction trajectory from **1** to the products by IRC computations [22, 23]. This revealed that the extension of the CH bonds and the formation of H–H are highly synchronized (Figure 2). The angular changes required to convert pyramidal methyl groups to planar methylene groups were also synchronized in that the two methyl hydrogens that were near the skeletal plane first moved away from that plane, reversed direction near the transition state, and finally returned to close to the skeletal plane pointing opposite to the interior CH and NH bonds. The two remaining methyl hydrogens moved steadily from being outside the skeletal plane to being in it.

Isotope Effects

Sizeable and similar isotope effects on the losses of (H,D)$_2$ from deuterated forms of **1** provide independent evidence that the C–H bonds are broken to similar degrees at the transition state for H$_2$-elimination [8, 9]. $CD_3CH=NH^+CH_3$ eliminates H$_2$ and HD in the ratio

36:64 [8]. Therefore, the positional integrity of the hydrogens in the methyl group attached to carbon is eroded; our calculations show that this is through the high-energy configuration $^+CH_2CH_2NHCH_3$ (see below). If the three deuterium and one protium atom of the original CD_3CH- entity became randomly distributed, H$_2$ and HD loss would be expected in the ratio 25:75 in the absence of isotope effects. Dividing 36/64 by 25/75 gives a lower limit of 1.69 for the isotope effect, favoring cleavage of a C–H rather than a C–D bond in this elimination. If the redistribution of hydrogen/deuterium atoms in the $-CHCD_3$ subgroup does not become statistical before dissociation, there would be a residual preference for inclusion of a deuterium atom in the eliminated hydrogen, thus favoring HD loss. Any incomplete exchange would lower the observed/predicted ratio such that the actual isotope effect would be greater than its lower limit of ca. 1.69:1. The loss of H$_2$ and HD in the ratio 43:57 from $CH_3CH=NH^+CHD_2$ (a ratio of 33:67 would be expected in the absence of any isotope effect), indicates an isotope effect of 1.5:1 (assuming zero exchange) on the cleavage of a CD bond in the N-methyl. The similar magnitude of the isotope effects on the two CH bond cleavages demonstrates that those bonds are breaking nearly simultaneously at the transition state, although the isotope effect for fission of the bond to the β-carbon atom may be larger than the lower limit of 1.4 obtained in the early investigation of $CD_3CH=NH^+CH_3$ [8]. The evidence of the isotope effects that the two bonds are broken to a similar extent at the transition state corroborates indications of our geometries obtained by theory,

Table 2. Energies for $CH_3CH=N^+HCH_3 \rightarrow CH_2=CHN^+H=CH_2 + H_2$ (kJ mol^{-1})

Species	B3LYP/6-31G(d)	B3LYP/6-311g(d,p)	QCISD/6-31G(d)	QCISD(T)/6-311G(d,p)
Cis-**1**	0	0	0	0
Trans-**1**	-7.4	-7.0	-7.9	-7.5
TS, cis/ trans **1**	251.9	249.8	267.3	263.5
TS(H$_2$ loss)	276.7	266.2	315.6	281.9
s-cis **2** + H$_2$	182.6	173.3	169.6	169.7
s-trans **2** + H$_2$	167.8	158.7	160.2	159.9
TS(**1** → **1**′)		275.6		279.0

Table 3. CH distances (Å) at the transition state for H-exchange between adjacent carbons in CH$_3$CH=NH$^+$CH$_3$

	CH bond[a]			
Theory level	C^{1}H^1	C^{1}H^2	C^{2}H^1	C^{2}H^2
B3LYP/6-31G(d)	1.1278	1.1242	1.9867	2.0015
B3LYP./6-311G(d,p)	1.1273	1.1246	1.9796	1.9893
QCISD/6-311G(d,p)	1.0955	1.1431	2.1596	1.8355

[a]The carbons and hydrogens involved are those of the C^{2}H$^2_3$C^{1}H^1-moiety.

establishing that H$_2$-elimination from **1** is quite synchronous.

Influence of Orbital Symmetry

Conservation of orbital symmetry in concerted chemical reactions [2] allows 1,4-H$_2$-elimination from **1** to be synchronized. To apply that theory, one compares the molecular orbitals of the separated fragments to see if the highest occupied molecular orbital of each can feed electron density into the lowest unoccupied molecular orbital of the other. This is possible at both termini only if the symmetries of the orbitals match, i.e., the phases of the wave function, have the same sign at the positions where the new bonds are to be formed. If the phases do not match, the reaction cannot be synchronous. That the phases match for the HOMO and LUMO at the transition state for H$_2$-elimination from **1** is illustrated in Figure 3, in which the orbitals are drawn to reflect electron density distributions derived from our computations.

H/D Exchange

H/D exchange was observed in the CD$_3$CH$-$ group of labeled **1** by Uccella and coworkers [8] in their initial study of H$_2$-elimination from **1**. To determine whether this exchange occurs by 1,2-H-shifts and, if so, the degree to which those shifts are or are not synchronized, we characterized them by theory. CH distances between breaking and forming bonds found by several levels of theory are given in Table 3. We found that H-exchange can indeed occur by 1,2-H-shifts between adjacent carbons. In this reaction, an H from the second carbon shifts to the first carbon almost completely by the point at which the shift of a hydrogen in the opposite direction is just beginning. No stable minimum was encountered in IRC tracing between **1** and **1**′ (B3LYP/6-31G{d} and B3LYP/6-311G{d,p} theories), so this exchange is concerted, although highly asynchronous. At the transition state, the distances from the migrating hydrogens to the same carbon atom were very similar according to the B3LYP theories, but differ by as

much as 0.3 Å for the longer bonds by QCISD theory. Thus, the transition state has a close resemblance to a primary carbocation. The energy of this transition state, (279 kJ mol^{-1} by B3LYP/6-311G{d,p} theory), is close to that of the transition state for H$_2$-elimination (266 kJ mol^{-1} at the same level of theory). This predicts exchange at the threshold for H$_2$-elimination, as occurs [8].

CH$_2$H$^\beta$CH=NH$^+$CH$_3$ (**1**) → $^+$CH$_2$CHH$^\beta$NHCH$_3$ → CH$_3$CH$^\beta$=NH$^+$CH$_3$ (**1**′).
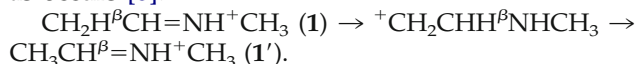
Summary

Theory demonstrates that the 1,4-elimination of H$_2$ from CH$_3$CH=N$^+$HCH$_3$ is concerted and highly synchronized over the course of the reaction, as required to conserve orbital symmetry. This reaction by **1**, **3–7** is a highly unusual, perhaps unique, in its synchronized breaking of two sigma bonds and formation of a π and σ bond. It is known only for immonium ions containing the H-CC=N$^+$CH structure. It differs fundamentally from 1,2-H$_2$-eliminations from species such as CH$_2$=N$^+$H$_2$ and CH$_3$CH$_3{}^+$, which tend to be highly asynchronous [1], presumably to circumvent orbital symmetry constraints.

References

1. Uggerud, E. Translational Energy Release: Experiment and Theory. H$_2$-Elimination Reactions of Small Gas Phase Ions and Correspondence to H–H Bond Activation. *Mass Spectrom. Rev.* **1999**, *18*, 285–308.
2. Woodward, R. B.; Hoffmann, R. The conservation of orbital symmetry. *Angew. Chem. Int. Ed.* **1969** *8*, 781–932.
3. Wendelboe, J. F.; Bowen, R.D.; Williams, D. H. Unimolecular Reactions of Ionized Alkanes. *J. Am. Chem. Soc.* **1981**, *103*, 2333–2339.
4. McAdoo, D. J.; Bowen, R. D. Alkane Eliminations from Ions in the Gas Phase. *Eur. Mass Spectrom.* **1999** *5*, 389–400.
5. Williams, D. H.; Hvistendahl, G. Kinetic Energy Release in Relation to Symmetry—Forbidden Reactions. *J. Am. Chem. Soc.* **1974**, *96*, 6753–6757.
6. Williams, D. H.; Hvistendahl, G. Kinetic Energy Release as a Mechanistic Probe. The Role of Orbital Symmetry. *J. Am. Chem. Soc.* **1974**, *96*, 6755–6757.
7. Øiestad, Å. M. L.; Uggerud, E. Loss of H$_2$ from CH$_2$NH$_2{}^+$ and NHNH$_2{}^+$. Reaction Mechanisms and Dynamics from Observation of Metastable Ion Fragmentation and ab Initio Calculations. *Int. J. Mass Spectrom. Ion Processes* **1997**, *167/168*, 117–126.
8. Uccella, N. A.; Howe, I.; Williams, D. H. Structure and Isomerization of Gaseous C$_3$H$_8$N$^+$ Metastable Ions. *J. Chem. Soc. B* **1971**, 1933–1939.
9. Bowen, R. D. The Chemistry of C$_n$H$_{2n+2}$N$^+$ ions. *Mass Spectrom. Rev.* **1991**, *10*, 225–279.
10. Dewar, M. J. S. Multibond Reactions Cannot Normally be Synchronous. *J. Am. Chem. Soc.* **1984**, *106*, 209–219.
11. McKee, M. L.; Shevlin, P. B.; Rzepa, H. S. Concerted Dihydrogen Exchange Between Methanol and Formaldehyde. A Theoretical Study. *J. Am. Chem. Soc.* **1986**, *108*, 5793–5798.
12. Olivella, S.; Solé, A.; McAdoo, D. J.; Griffin, L. L. Unimolecular Reactions of Ionized Alkanes: Theoretical Study of the Potential Energy Surface for CH$_3$. and CH$_4$ Losses from Ionized Butane and Isobutane. *J. Am. Chem. Soc.* **1994**, *116*, 11078–11088.
13. Olivella, S.; Solé, A.; McAdoo, D. J. Methane Elimination from Ionized Propane Through an Ion-Neutral Complex: An Ab Initio Study. *J. Am. Chem. Soc.* **1996**, *118*, 9368–9376.
14. Hudson, C. E.; McAdoo, D. J. Characterization by Theory of H-Transfers and Onium Reactions of CH$_3$CH$_2$CH$_2$N$^+$H=CH$_2$. *J. Am. Soc. Mass Spectrom.* **2007**, *18*, 270–278.
15. Hudson, C. E.; McAdoo, D. J. Ethene-Elimination from CH$_3$CH$_2$NH=CH$_2{}^+$: Reaction Pathways at the Boundary Between Stepwise and Concerted Processes. *J. Am. Soc. Mass Spectrom.* **1998**, *9*, 138–148.
16. Hudson, C. E.; McAdoo, D. J. Methane Loss from (CH$_3$)$_3$O$^+$: An Asynchronous, Concerted 1,2-Alkane Elimination. *Int. J. Mass Spectrom.* **2006**, *248*, 103–107.
17. Traeger, J. C.; Hudson, C. E.; McAdoo, D. J. A Photoionization Study of the Ion-Neutral Complexes [CH$_3$CH$^+$CH$_3$, CH$_2$CH$_3$] and [CH$_3$CH$_2$CH $^+$CH$_3$, CH$_3$] in the Gas Phase: Formation, H-transfer, and C–C Bond

Formation Between Partners, and Channeling of Energy into Dissociation. *J. Am. Soc. Mass Spectrom.* **1996**, *7*, 73–81.
18. Tramontini, M. Advances in the Chemistry of Mannich Bases. *Synthesis* **1973**, *12*, 703–775.
19. Dyke, S. F. The Chemistry of Enamines; Cambridge University Press: London, 1973;
20. Frisch, M. J.; Trucks, G. W.; Schlegel, H. B.; Scuseria, G. E.; Robb, M. A.; Cheeseman, J. R.; Montgomery, J. A., Jr.; Vreven, T.; Kudin, K. N.; Burant, J. C.; Millam, J. M.; Iyengar, S. S.; Tomasi, J.; Barone, V.; Mennucci, B.; Cossi, M.; Scalmani, G.; Rega, N.; Petersson, G. A.; Nakatsuji, H.; Hada, M.; Ehara, M.; Toyota, K.; Fukuda, R.; Hasegawa, J.; Ishida, M.; Nakajima, T.; Honda, Y.; Kitao, O.; Nakai, H.; Klene, M.; Li, X.; Knox, J. E.; Hratchian, H. P.; Cross, J. B.; Adamo, C.; Jaramillo, J.; Gomperts, R.; Stratmann, R. E.; Yazyev, O.; Austin, A. J.; Cammi, R.; Pomelli, C.; Ochterski, J. W.; Ayala, P. Y.; Morokuma, K.; Voth, G. A.; Salvador, P.; Dannenberg, J. J.; Zakrzewski, V. G.; Dapprich, S.; Daniels, A. D.; Strain, M. C.; Farkas, O.; Malick, D. K.; Rabuck, A. D.; Raghava-chari, K.; Foresman, J. B.; Ortiz, J. V.; Cui, Q.; Baboul, A. G.; Clifford, S.; Cioslowski, J.; Stefanov, B. B.; Liu, G.; Liashenko, A.; Piskorz, P.;

Komaromi, I.; Martin, R. L.; Fox, D. J.; Keith, T.; Al-Laham, M. A.; Peng, C. Y.; Nanayakkara, A.; Challacombe, M.; Gill, P. M. W.; Johnson, B.; Chen, W.; Wong, M. W.; Gonzalez, C.; Pople, J. A. Gaussian 03; Revision B.04, Gaussian, Inc.: Pittsburgh, PA, 2003.
21. Scott, A. P.; Radom, L. Harmonic Vibrational Frequencies: An Evalua-tion of Hartree-Fock, Møller-Plesset, Quadratic Configuration Interac-tion, Density Functional Theory, and Semiempirical Scale Factors. *J. Phys. Chem.* **1996**, *100*, 16502–16513.
22. Gonzalez, C.; Schlegel, H. B. An Improved Algorithm for Reaction Path Following. *J. Chem. Phys.* **1989**, *90*, 2154–2161.
23. Gonzalez, C.; Schlegel, H. B. Reaction Path Following in Mass-Weighted Internal Coordinates. *J. Phys. Chem.* **1990**, *94*, 5523–5527.
24. Kao, J. A Molecular Orbital Based Molecular Mechanics Approach to Study Conjugated Hydrocarbons. *J. Am. Chem. Soc.* **1987**, *109*, 3817–3829.
25. Anslyn, E. V.; Dougherty, D. A. Modern Physical Organic Chemistry; University Science Books: Sausalito, CA, 2004; p 115